Global Tracking Control of Underactuated Ships With Input and Velocity Constraints Using Dynamic Surface Control Method

Dongkyoung Chwa

***Abstract*—This paper proposes a global tracking control method for underactuated ships with input and velocity constraints using the dynamic surface control (DSC) method, where the control structure is formed in a modular way that cascaded kinematic and dynamic linearizations can be achieved similarly as in the backstepping method. First, the first step linearization of the kinematics determines the pseudo (or auxiliary) surge velocity and yaw angle, which are used as the commands for the second-step linearization. Then, in the second-step linearization of dynamics, the actual torque inputs are designed to make the actual surge velocity and yaw angle follow these pseudo commands to achieve the position and yaw angle tracking. By employing the dynamic surface control method in the design of each kinematic and dynamic linearization law, we can obtain a control structure that is much simpler than the previous backstepping-based controllers such that it is beneficial from the practical application viewpoint. In addition, it is possible to track general reference trajectories, i.e., the reference yaw velocity need not be persistently exciting and there is no restriction on the initial yaw tracking error. In particular, global tracking control is achieved even in the presence of input and velocity constraints, unlike the DSC method which introduces the several filters in the backstepping design procedure to avoid the model differentiation and make it easier to be implemented and usually has semiglobal tracking performance. Finally, the stability analysis and numerical simulations are performed to confirm the effectiveness of the proposed scheme.**

***Index Terms*—Dynamic surface control (DSC), input/velocity constraints, semiglobal tracking, tracking control, underactuated ships.**

I. Introduction

MUCH research has been done on the control of underactuated mechanical systems, which are systems with fewer independent actuators than degrees of freedom [1]. An example of these is nonholonomic systems. The controller design for these kinds of systems is meaningful from both theoretical and practical viewpoints in that: 1) well-known Brockett's necessary condition in [2] has shown that asymptotic stabilization of the nonholonomic system cannot be achieved with a time-invariant continuous controller and 2) the underactuated control system can handle actuator failure and, thus, can be practically employed in many systems.

In addition to the underactuated systems with nonholonomic velocity constraints (e.g., two-wheeled mobile robots [3]–[5]), there are also underactuated systems with constraints given in terms of generalized coordinates and their first- and second-order derivatives (velocities and accelerations) (e.g., underactuated rigid spacecrafts [6]–[10] and underactuated ships [11]–[20]). In particular, since mobile robots can be transformed into a chained form, a recursive technique in [22] can be used for the tracking controller as in [3]. However, the underactuated ship cannot be transformed into a driftless chained system [11]. Therefore, the control approach applied to the mobile robot control cannot be directly employed in an underactuated ship control, which makes it more challenging to control the underactuated ship.

In addition, it is shown in [12] that the underactuated ship cannot be asymptotically stabilized by a continuous time-invariant feedback law. Accordingly, the control of underactuated surface ships with only surge force and yaw moment as control inputs has attracted much attention. A continuous time-invariant state controller was designed to achieve global exponential position tracking in [13], but yaw angle could not yet be controlled. It should be noted here that similar work is done in [23], not for the underactuated ship, but for the wheeled mobile robots in the presence of skidding and slippling. Global tracking results were continued in the following literatures. In [14], a coordinate transformation was used to give a triangular-like form, and a recursive integrator backstepping method for the chained system was employed to give the local global exponential practical tracking results. Whereas the work in [15] and [16] used cascading approach, the work in [17] used Lyapunov's direct method for global tracking. All of these results, however, assume that the reference yaw velocity does not converge to zero and requires persistent excitation condition, implying that it is impossible to track a straight-line reference trajectory. This assumption was eliminated in the tracking problem in [18], and then in both stabilization and tracking in [19] and [20]. However, these trajectory tracking controllers were found to be quite dependent on the reference model and much more complicated, making its applicability dubious since its computational effort is too large for real-time implementation. Accordingly, a simpler algorithm that is less dependent on the reference trajectory should be developed, as noted in [21]. On the other hand, the path following result in [21] requires the assumption that the yaw tracking error is less than 0.5π. However, this significantly

Manuscript received May 26, 2010; accepted August 08, 2010. Manuscript received in final form October 27, 2010. Date of publication December 10, 2010; date of current version September 16, 2011. This work was supported by the Korea Government (MEST) under Korea Science and Engineering Foundation(KOSEF) Grant 2009-0069742 . Recommended by Associate Editor S. Devasia.

The author is with the Department of Electrical and Computer Engineering, Ajou University, Suwon 443-749, Korea (e-mail: dkchwa@ajou.ac.kr).

Digital Object Identifier 10.1109/TCST.2010.2090526

1063-6536/$26.00 © 2010 IEEE

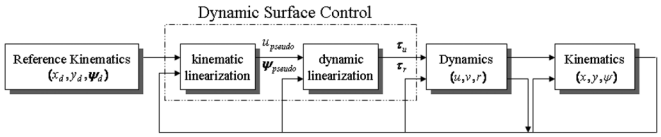

Fig. 1. DSC for posture tracking of underactuated ships.

restrict the class of reference paths (or trajectories) to be used for practical application. On the other hand, whereas an underactuated ship moves in the open sea by maintaining the limited forward velocity and angular velocity, there have been few practical studies on the ship control considering the input and velocity constraints.

Thus, we need to develop a much simpler and modular control structure, requiring much less computational effort and providing the possibility of employing the various types of dynamic controllers along with the rigorous stability analysis, such that it is beneficial from the practical application viewpoint. In addition, it should achieve satisfactory trajectory tracking performance, with no restriction on the reference trajectory (that is, the reference yaw velocity does not need to be persistently exciting and a whole range of the initial yaw angle is possible). Finally, it should satisfy the input and velocity constraints of the underactuated ship.

To this end, we employ a dynamic surface control method in the proposed controller (see Fig. 1), which has been much studied in [24]; the idea of backstepping is used, but the complexity coming from the backstepping is avoided by applying the low-pass filters in the design of the cascaded modular kinematic and dynamic control laws via kinematic and dynamic linearization methods. In this scheme, the pseudo (or auxiliary) surge and sway velocities are obtained, and these are transformed into pseudo surge velocity and yaw angle. Then, the actual torque inputs are designed to make the actual surge velocity and yaw angle follow the pseudo velocity and yaw angle. Unlike the dynamic surface control (DSC) method, where the semiglobal ultimate boundedness is obtained [24], [25], the proposed method gives the global ultimate boundedness even in the presence of input and velocity constraints, as will be shown later in Theorem 1. In particular, it should be noted that a fully actuated ship, not an underactuated ship, is handled in [25], and, thus, it becomes much easier to control. The stability analysis and simulations are performed to evaluate the tracking performance for reference trajectories such as sinusoidal curves, circles, straight lines, and a combination of these trajectories. As demonstrated in simulations given later and also noticed in [26], robustness against uncertainties can be improved using the hierarchical approach. We could see that the position and yaw angle tracking can be achieved with relatively small errors for various reference trajectories.

II. Kinematics and Dynamics of Underactuated Ships

Here, we briefly describe the kinematics and dynamics of underactuated ships. The general six-degree-of-freedom (6-DOF) ship model can be reduced to the motion in surge, sway, and yaw under the following assumptions: 1) the heave, roll, and pitch modes induced by wave, wind, and currents drift forces can be neglected; 2) the inertia, added mass, and hydrodynamic damping matrices are diagonal, which holds good for ships having port/starboard and fore/aft symmetry; and 3) available controls are surge force τ_u and yaw moment τ_r. Then, as in [27], the kinematic and dynamic models can be given by

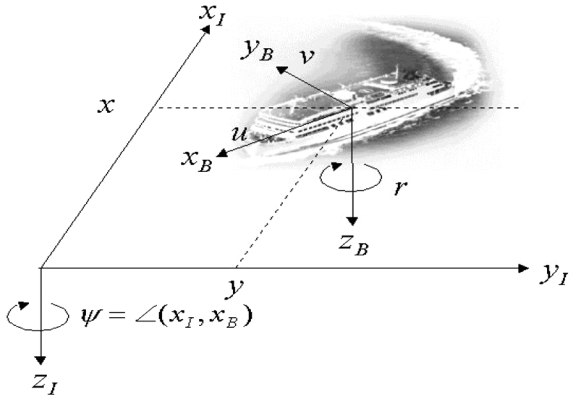

Fig. 2. Earth-fixed (x_I, y_I, z_I) and body-fixed coordinate systems (x_B, y_B, z_B).

$$\begin{cases} \dot{x} = u\cos(\psi) - v\sin(\psi) \\ \dot{y} = u\sin(\psi) + v\cos(\psi) \\ \dot{\psi} = r \end{cases} \tag{1}$$

$$\begin{cases} \dot{u} = \frac{m_2}{m_1}vr - \frac{d_1}{m_1}u + \frac{1}{m_1}\tau_u \\ \dot{v} = -\frac{m_1}{m_2}ur - \frac{d_2}{m_2}v \\ \dot{r} = \frac{(m_1 - m_2)}{m_3}uv - \frac{d_3}{m_3}r + \frac{1}{m_3}\tau_r. \end{cases} \tag{2}$$

Here, x and y are positions and ψ is the yaw angle of the ship in the earth-fixed frame, u and v are linear velocities in surge (body-fixed x-direction) and sway (body-fixed y-direction), and r is angular velocity in yaw (body-fixed z-direction) (see Fig. 2), and the parameters $m_i > 0$ are ship inertia including added mass effects, and $d_i > 0$ are hydrodynamic damping in surge, sway, and yaw, for $i = 1$, 2, and 3, respectively. As there is limitation on the input and velocity of the actual ship, we make the following assumption.

Assumption 1: There exist constraints on the control inputs and velocities as $|\tau_u| \le \tau_{u\max}$, $|\tau_r| \le \tau_{r\max}$, $|u| \le u_{\max}$, $|v| \le v_{\max}$, and $|r| \le r_{\max}$ for positive constants $v_{\max}$ and $r_{\max}$.

Unlike the wheeled mobile robot, the time derivatives of surge and sway displacement in (1) contain the sway velocity components, and the second equation in (2) shows that this sway velocity decreases to zero only when the surge velocity u or the angular velocity r remains zero. Thus, the control law for the mobile robot cannot be directly employed to the ship model, and the sway motion must be considered in the design of the ship control law.

III. Tracking Control Using DSC

The control objective is to steer the ship so that it follows the reference trajectory using the DSC method, even in the presence of input and velocity constraints. In contrast to backstepping or recursive methods [15]–[20], which results in the complicated control structure due to the explosion of terms involving the calculation of the state derivatives, the proposed method described in Fig. 1 results in the simpler and modular control structure, in

such a way that the desired surge velocity and yaw angle are determined and then the actual torque inputs are designed to make the actual velocity and yaw angle follow the desired velocity and angle, respectively. The detailed description on this will be given in this section.

Using the expressions in (1) and (2), we can have a reference trajectory given by

$$\begin{cases} \dot{x}_d = u_d\cos(\psi_d) - v_d\sin(\psi_d) \\ \dot{y}_d = u_d\sin(\psi_d) + v_d\cos(\psi_d) \\ \dot{\psi}_d = r_d \end{cases} \tag{3}$$

$$\begin{cases} \dot{u}_d = \frac{m_2}{m_1}v_d r_d - \frac{d_1}{m_1}u_d + \frac{1}{m_1}\tau_{ud} \\ \dot{v}_d = -\frac{m_1}{m_2}u_d r_d - \frac{d_2}{m_2}v_d \\ \dot{r}_d = \frac{(m_1-m_2)}{m_3}u_d v_d - \frac{d_3}{m_3}r_d + \frac{1}{m_3}\tau_{rd} \end{cases} \tag{4}$$

where x_d and y_d are positions of the reference, respectively, ψ_d is yaw angle of the reference in the earth-fixed frame, u_d and v_d are reference linear velocities in surge (body-fixed x-direction) and sway (body-fixed y-direction), r_d is the reference angular velocity in yaw (body-fixed z-direction), and τ_{ud} and τ_{rd} are reference surge force and yaw moment, respectively. Here, it is natural from Assumption 1 and the argument given later to make the following assumption.

Assumption 2: The reference velocities u_d, v_d, and r_d satisfy $|u_d| + |v_d| < u_{\max}$ and $|r_d| < r_{\max}$.

Here, we define the posture tracking errors and velocity errors as

$$x_e := x - x_d \quad y_e := y - y_d \quad \psi_e := \psi - \psi_d \tag{5a}$$

$$u_e := u - u_d \quad v_e := v - v_d \quad r_e := r - r_d. \tag{5b}$$

In the following, control inputs (τ_u, τ_r) will be designed in order to reduce the posture tracking errors (x_e, y_e, ψ_e) to zero.

The first two rows in (1) and (3) can be used to obtain

$$\dot{x}_e + k_p\tanh(\overline{k}_p x_e) = X \tag{6a}$$

$$\dot{y}_e + k_p\tanh(\overline{k}_p y_e) = Y \tag{6b}$$

where

$$\begin{aligned} X :=\ & u\cos(\psi) - v\sin(\psi) - u_d\cos(\psi_d) + v_d\sin(\psi_d) \\ & + k_p\tanh(\overline{k}_p x_e) \end{aligned} \tag{7a}$$

$$\begin{aligned} Y :=\ & u\sin(\psi) + v\cos(\psi) - u_d\sin(\psi_d) - v_d\cos(\psi_d) \\ & + k_o\tanh(\overline{k}_p y_e) \end{aligned} \tag{7b}$$

for $k_p, \overline{k}_p > 0$. It should be noted here that k_p needs to be adjusted later, as in (15), such that the constraint on the forward velocity can be satisfied. Equations (6a) and (6b) show that the position tracking can be achieved by reducing X and Y to zero. To this end, first, the variables X and Y in (7a) and (7b) are arranged as

$$\begin{aligned} X =\ & \{u\cos(\psi_e) - v\sin(\psi_e) - u_d\}\cos(\psi_d) \\ & - \{u\sin(\psi_e) + v\cos(\psi_e) - v_d\}\sin(\psi_d) + k_p\tanh(\overline{k}_p x_e) \\ Y =\ & \{u\cos(\psi_e) - v\sin(\psi_e) - u_d\}\sin(\psi_d) \\ & + \{u\sin(\psi_e) + v\cos(\psi_e) - v_d\}\cos(\psi_d) + k_p\tanh(\overline{k}_p y_e) \end{aligned}$$

which can be rewritten as

$$\begin{aligned} & \begin{pmatrix} \cos(\psi_d) & -\sin(\psi_d) \\ \sin(\psi_d) & \cos(\psi_d) \end{pmatrix}^{-1} \begin{pmatrix} X \\ Y \end{pmatrix} \\ & \qquad = \begin{pmatrix} u\cos(\psi_e) - v\sin(\psi_e) - \overline{X} \\ u\sin(\psi_e) + v\cos(\psi_e) - \overline{Y} \end{pmatrix} \end{aligned} \tag{8}$$

where

$$\begin{aligned} \overline{X} =\ & u_d - \cos(\psi_d)k_p\tanh(\overline{k}_p x_e) \\ & - \sin(\psi_d)k_p\tanh(\overline{k}_p y_e) \end{aligned} \tag{9a}$$

$$\begin{aligned} \overline{Y} =\ & v_d + \sin(\psi_d)k_p\tanh(\overline{k}_p x_e) \\ & - \cos(\psi_d)k_p\tanh(\overline{k}_p y_e). \end{aligned} \tag{9b}$$

Then, the proper values of u and v are required to achieve the convergence of the right-hand side of (8), i.e.,

$$\tilde{x}_e := u\cos(\psi_e) - v\sin(\psi_e) - \overline{X} \tag{10a}$$

$$\tilde{y}_e := u\sin(\psi_e) + v\cos(\psi_e) - \overline{Y} \tag{10b}$$

to zero, which implies the convergence of

$$\cos(\psi_e)\tilde{x}_e + \sin(\psi_e)\tilde{y}_e = u - \cos(\psi_e)\overline{X} - \sin(\psi_e)\overline{Y} \tag{11a}$$

$$-\sin(\psi_e)\tilde{x}_e + \cos(\psi_e)\tilde{y}_e = v + \sin(\psi_e)\overline{X} - \cos(\psi_e)\overline{Y} \tag{11b}$$

to zero, since (11) can be obtained when the appropriate matrix is multiplied to both sides of (10).

Later in the derivation of Lemma 1, the boundedness of $\overline{X}$ and $\overline{Y}$ in (9) resulting from the use of hyperbolic tangent functions can be effectively used.

Remark 1: We can see from (9) and (10) that, when the posture tracking errors become zero, $(x_e = y_e = \psi_e = \tilde{x}_e = \tilde{y}_e = 0)$, u_e and v_e also become zero naturally.

Suppose that we can determine u_{pseudo} and v_{pseudo} (the pseudo commands for u and v) from (11) and then determine τ_u and τ_r such that u and v follow u_{pseudo} and v_{pseudo} as in (12) and (31), respectively. In this case, position tracking can be achieved, but yaw angle tracking is not guaranteed. In other words, position tracking in the opposite direction can occur in this situation. Thus, we will determine the pseudo surge velocity u_{pseudo} and pseudo yaw angle ψ_{pseudo} as commands for the dynamic linearization to have the position tracking in the right direction, such that both position tracking and yaw angle tracking can be achieved. This is also natural in the sense that u and ψ can be controlled directly as can be seen in the dynamic model (2).

First, u_{pseudo} can be readily determined as

$$u_{\text{pseudo}} = \cos\left((\psi_e)_{\text{pseudo}}\right)\overline{X} + \sin\left((\psi_e)_{\text{pseudo}}\right)\overline{Y} \tag{12}$$

to make (11a) equal to zero when $\psi_e = (\psi_e)_{\text{pseudo}}$, where $(\psi_e)_{\text{pseudo}}$ (the pseudo commands for ψ_e) is determined later in (17). Here, note that ψ_{pseudo} (the pseudo commands for ψ) can be obtained using the definition of ψ_e in (5a) as

$$\psi_{\text{pseudo}} = (\psi_e)_{\text{pseudo}} + \psi_d. \tag{13}$$

Substitution of (9) into (12) gives

$$\begin{aligned}|u_{\text{pseudo}}| &= \Big|\cos\Big((\psi_e)_{\text{pseudo}}\Big)\,u_d + \sin\Big((\psi_e)_{\text{pseudo}}\Big)\,v_d \\ &\quad + \Big\{-\cos\Big((\psi_e)_{\text{pseudo}}\Big)\cos(\psi_d) \\ &\qquad + \sin\Big((\psi_e)_{\text{pseudo}}\Big)\sin(\psi_d)\Big\} \\ &\quad \cdot k_p \tanh(\overline{k}_p x_e) \\ &\quad + \Big\{-\cos\Big((\psi_e)_{\text{pseudo}}\Big)\sin(\psi_d) \\ &\qquad - \sin\Big((\psi_e)_{\text{pseudo}}\Big)\cos(\psi_d)\Big\} \\ &\quad \cdot k_p \tanh(\overline{k}_p y_e)\Big| \\ &= \Big|\cos\Big((\psi_e)_{\text{pseudo}}\Big)\,u_d + \sin\Big((\psi_e)_{\text{pseudo}}\Big)\,v_d \\ &\quad - \{\cos(\psi_{\text{pseudo}})\tanh(\overline{k}_p x_e) \\ &\qquad + \sin(\psi_{\text{pseudo}})\tanh(\overline{k}_p y_e)\}\,k_p\Big| \\ &\le |u_d| + |v_d| + \sqrt{2}k_p. \end{aligned} \tag{14}$$

Considering Assumption 1, u_{pseudo} should satisfy $|u_{\text{pseudo}}| \le u_{\max}$. Thus, from (14) and Assumption 2, k_p should be adjusted to satisfy

$$0 \le k_p \le k_{p\max} := \frac{u_{\max} - |u_d| - |v_d|}{\sqrt{2}}. \tag{15}$$

Second, to determine ψ_{pseudo}, $\tilde{x}_e$ and $\tilde{y}_e$ in (10) are modified by combining sine and cosine functions as

$$\tilde{x}_e = \sqrt{u^2+v^2}\cos(\psi_e+\varphi) - \overline{X} \tag{16a}$$

$$\tilde{y}_e = \sqrt{u^2+v^2}\sin(\psi_e+\varphi) - \overline{Y} \tag{16b}$$

where $\varphi := \text{atan2}(v,u)$, $\text{atan2}(v,u)$ is a four-quadrant inverse tangent with the values in the interval of $(-\pi,\pi]$. If we let $\tilde{x}_e = \tilde{y}_e = 0$ in (16), then we can have $\tan(\psi_e+\varphi) = \overline{Y}/\overline{X}$. From this, $(\psi_e)_{\text{pseudo}}$ can be determined as either

$$(\psi_e)_{\text{pseudo}} = \theta - \varphi \tag{17a}$$

or

$$(\psi_e)_{\text{pseudo}} = \pi + \theta - \varphi \tag{17b}$$

where $\theta := \text{atan2}(\overline{Y},\overline{X})$. Here, $(\psi_e)_{\text{pseudo}}$ should be determined between (17a) and (17b) depending on the sign of u_d, such that u and u_d have the same sign. This is because forward (respectively, backward) motion of the reference trajectory should be achieved in the case that the sign of u_d is positive (resp. negative). To this end, (12) is expressed as

$$u_{\text{pseudo}} = \cos\Big((\psi_e)_{\text{pseudo}} - \theta\Big)\sqrt{\overline{X}^2 + \overline{Y}^2} \tag{18}$$

which is positive for $|(\psi_e)_{\text{pseudo}} - \theta| < \pi/2$ and negative for $|\pi - ((\psi_e)_{\text{pseudo}} - \theta)| < \pi/2$. Accordingly, in the case of positive u_d, we should have (17a), which satisfies $|(\psi_e)_{\text{pseudo}} - \theta| \le \pi/2$ since $|\tan^{-1}(\cdot)| \le \pi/2$. Thus, u_{pseudo} becomes positive. Similarly, in the case of negative u_d, we should have (17b) to have negative u_{pseudo}. In summary, when $u = u_{\text{pseudo}}$ in (12) and $\psi = \psi_{\text{pseudo}}$ in (13) are satisfied, position and yaw angle tracking can be achieved.

Finally, we need to design the control inputs τ_u and τ_r to make u and ψ follow u_{pseudo} and ψ_{pseudo}. Backstepping or recursive design involves (first- and second-order) time derivatives of ψ_{pseudo}, which results in a complicated control structure such that much computational effort is needed. Thus, instead of adopting these methods, we will design a dynamic surface control law using the fact that u- and ψ-dynamics can be controlled by τ_u and τ_r, which is given by

$$\tau_u = m_1\left\{-\frac{m_2}{m_1}vr + \frac{d_1}{m_1}u + \overline{\tau}_u\right\} \tag{19a}$$

$$\tau_r = m_3\left\{-\frac{(m_1-m_2)}{m_3}uv + \frac{d_3}{m_3}r + \overline{\tau}_r\right\} \tag{19b}$$

such that

$$\dot{u} = \overline{\tau}_u, \quad \dot{r} = \overline{\tau}_r \quad (\text{i.e., } \ddot{\psi} = \overline{\tau}_r). \tag{20}$$

Here, we introduce the following definition as in [24]:

$$E_u = u - u_{\text{pseudo}}, \quad T_u\dot{u}_{cmd} = -u_{cmd} + u_{\text{pseudo}},$$
$$\overline{E}_u = u - u_{cmd} \tag{21a}$$

$$E_\psi = \psi - \psi_{\text{pseudo}}, \quad T_\psi\dot{\psi}_{cmd} = -\sin(\psi_{cmd} - \psi_{\text{pseudo}}),$$
$$\overline{E}_\psi = \psi - \psi_{cmd} \tag{21b}$$

$$E_r = r - r_{\text{pseudo}}, \quad T_r\dot{r}_{cmd} = -r_{cmd} + r_{\text{pseudo}},$$
$$\overline{E}_r = r - r_{cmd} \tag{21c}$$

where T_u, T_ψ, T_r are time constants of low-pass filters and

$$r_{\text{pseudo}} = -k_\psi\sin(\overline{E}_\psi/2) + \dot{\psi}_{cmd} \tag{22}$$

for a positive constant k_ψ. Combining (22) and (21b) gives

$$\left|r_{\text{pseudo}} + k_\psi\sin(\overline{E}_\psi/2)\right| = \frac{|\sin(\psi_{cmd} - \psi_{\text{pseudo}})|}{T_\psi}. \tag{23}$$

As r_{pseudo} should satisfy $|r_{\text{pseudo}}| \le r_{\max}$ considering Assumption 1, k_ψ can be chosen to satisfy (24a), and then T_ψ can be adjusted to satisfy

$$k_\psi < r_{\max} \tag{24a}$$

$$T_\psi \ge |\sin(\psi_{cmd} - \psi_{\text{pseudo}})| \Big/ \left(r_{\max} + \left|k_\psi\sin(\overline{E}_\psi/2)\right|\right). \tag{24b}$$

Then, $\overline{\tau}_u$ and $\overline{\tau}_r$ in (19a) and (19b) are given by

$$\overline{\tau}_u = -k_u\overline{E}_u + \dot{u}_{cmd} \tag{25a}$$

$$\overline{\tau}_r = -2\zeta k_r\overline{E}_r - k_r^2\sin(\overline{E}_\psi/2) + \dot{r}_{cmd} \tag{25b}$$

where k_u, k_r, and ζ are positive constants. Combining (19) and (25) gives

$$\begin{aligned}&|\tau_u + m_2vr - d_1u + m_1k_u\overline{E}_u| \\ &\quad = \frac{m_1|-u_{cmd}+u_{\text{pseudo}}|}{T_u} \end{aligned} \tag{26a}$$

$$\begin{aligned}&\left|\tau_r + (m_1-m_2)uv - d_3r + m_3\left\{2\zeta k_r\overline{E}_r + k_r^2\sin\left(\frac{\overline{E}_\psi}{2}\right)\right\}\right| \\ &\quad = \frac{m_3|-r_{cmd}+r_{\text{pseudo}}|}{T_r}. \end{aligned} \tag{26b}$$

Thus, k_u, k_r, T_u, and T_r should be adjusted such that the equations in (27), shown at the bottom of the page, are satisfied. Then, from (20), (21), (22), and (25), it follows that

$$\dot{\overline{E}}_u = -k_u \overline{E}_u \tag{28a}$$
$$\dot{\overline{E}}_\psi = r - \dot{\psi}_{cmd} = -k_\psi \sin(\overline{E}_\psi/2) + E_r \tag{28b}$$
$$\dot{\overline{E}}_r = \overline{\tau}_r - \dot{r}_{cmd} = -2\zeta k_r \overline{E}_r - k_r^2 \sin(\overline{E}_\psi/2). \tag{28c}$$

Remark 2: The assumption on the yaw angle tracking error as $|\psi_e| < 0.5\pi$ in [21] is not needed (cf. Scenario 3 in Section IV).

Remark 3: Since yaw angles ε and $2n\pi + \varepsilon$ are actually the same for the integer n, the discontinuity of the yaw angle is inevitable in the Cartesian coordinates. For example, when $\psi_{\text{pseudo}} = 2\pi - \varepsilon$ and $\psi = \varepsilon$, the clockwise rotation of 2ε angle is reasonable rather than counterclockwise rotation of $2\pi - 2\varepsilon$. As a sinusoidal function can avoid this problem, we introduce the sinusoidal function of $\overline{E}_\psi$ in (22). Note that in the case of the polar coordinates (R, θ, ψ), the relationship $(x, y, \psi) = (R\cos(\theta), R\sin(\theta), \psi)$ shows that the discontinuity of yaw angle is not present, whereas the singular problem around the origin appears (as R goes to zero).

The boundedness of the several state variables can be guaranteed in the following lemma.

Lemma 1 (Boundedness of the Velocities): The control inputs $\tau = [\tau_u \ \tau_r]^T$ in (19), (21), (22), and (25), where u_{pseudo} in (12) and ψ_{pseudo} in (13) and (17a) in the case of positive u_d (respectively, (13) and (17b) in the case of negative u_d) are used, achieve the boundedness of u, v, and r.

Proof: We will show the boundedness of each state variable in the following procedure.

1) *The boundedness of* u: as $\overline{X}$ and $\overline{Y}$ in (9a) and (9b) are bounded, u_{pseudo} in (12) is bounded, and thus, u_{cmd} and $\dot{u}_{cmd}$ are bounded from (21a). As $\overline{E}_u (= u - u_{cmd})$ converges to zero from (28a), u is bounded.
2) *The boundedness of* r: as $(\psi_e)_{\text{pseudo}}$ is bounded from its definition in (17), ψ_{pseudo} in (13) is also bounded. Then, the boundedness of ψ_{cmd} and $\dot{\psi}_{cmd}$ follows from (21b). Thus, 5fr_{pseudo} is bounded from (22), and $T_r \dot{r}_{cmd} = -r_{cmd} + r_{\text{pseudo}}$ in (21c) shows that r_{cmd} and $\dot{r}_{cmd}$ are bounded. From $\ddot{\psi} = \overline{\tau}_r$ and $\overline{\tau}_r$ in (25b),

$$\ddot{\psi} + 2\zeta k_r \dot{\psi} = 2\zeta k_r r_{cmd} - k_r^2 \sin(\overline{E}_\psi/2) + \dot{r}_{cmd} \tag{29}$$

holds. As the right-hand side of (29) is bounded, $\dot{\psi}$ and $\ddot{\psi}$ (i.e., r and $\dot{r}$) are bounded.
3) *The boundedness of* v: as u and r are bounded, the second row in (2) shows that v and $\dot{v}$ are bounded. (Q.E.D.)

The expression of v in the following lemma will be used later in Theorem 1.

Lemma 2 (Expression of v*):* The sway velocity v can be expressed as

$$v = v_{\text{pseudo}} + T_u(E_u) \tag{30}$$

where

$$v_{\text{pseudo}} = -\sin\Big((\psi_e)_{\text{pseudo}}\Big)\overline{X} + \cos\Big((\psi_e)_{\text{pseudo}}\Big)\overline{Y} \tag{31}$$
$$T_u(E_u) := \overline{T}_u E_u \tag{32}$$
$$\overline{T}_u := \frac{\cos\Big((\psi_e)_{\text{pseudo}}\Big)\overline{Y} - \sin\Big((\psi_e)_{\text{pseudo}}\Big)\overline{X}}{\cos\Big((\psi_e)_{\text{pseudo}}\Big)\overline{X} + \sin\Big((\psi_e)_{\text{pseudo}}\Big)\overline{Y}}. \tag{33}$$

Here, v_{pseudo}, $\overline{T}_u$ are bounded functions, and $\overline{T}_u$ is bounded by

$$|\overline{T}_u| \le \overline{T}_{u\max} := m_1 r_{\max}/d_2. \tag{34}$$

Also, as E_u decreases to zero, $T_u(E_u)$ decreases to zero, making v become v_{pseudo}.

Proof: As $(\psi_e)_{\text{pseudo}}$ in (17a) and (17b) satisfies

$$(\psi_e)_{\text{pseudo}} = \operatorname{atan2}(\overline{Y}, \overline{X}) - \operatorname{atan2}(v, u) \tag{35a}$$

or

$$(\psi_e)_{\text{pseudo}} = \pi + \operatorname{atan2}(\overline{Y}, \overline{X}) - \operatorname{atan2}(v, u) \tag{35b}$$

we have

$$\begin{aligned}\tan\Big((\psi_e)_{\text{pseudo}}\Big) &= \{\overline{Y}/\overline{X} - v/u\} / \{1 + (\overline{Y}/\overline{X}) \cdot (v/u)\} \\ &= (\overline{Y}u - \overline{X}v)/(\overline{X}u + \overline{Y}v)\end{aligned} \tag{36}$$

which results in

$$\begin{aligned}v &= \left\{\overline{Y} - \overline{X}\tan\Big((\psi_e)_{\text{pseudo}}\Big)\right\} \\ &\quad \Big/ \left\{\overline{X} + \overline{Y}\tan\Big((\psi_e)_{\text{pseudo}}\Big)\right\} \cdot u \\ &= \overline{T}_u u \\ &= \overline{T}_u u_{\text{pseudo}} + T_u(E_u).\end{aligned} \tag{37}$$

From the second row of (2), v can be seen as the low-pass-filtered value of ur (i.e., $|v| \le m_1|u|r_{\max}/d_2$), which along with the second equality of (37) leads to (34).

As v_{pseudo} in (31) can be expressed as

$$v_{\text{pseudo}} = -\sin\Big((\psi_e)_{\text{pseudo}} - \theta\Big)\sqrt{\overline{X}^2 + \overline{Y}^2} \tag{38}$$

$$T_u \ge \frac{m_1|-u_{cmd} + u_{\text{pseudo}}|}{\{\tau_{u\max} + |m_2 vr - d_1 u + m_1 k_u \overline{E}_u|\}} \tag{27a}$$
$$T_r \ge \frac{m_3|-r_{cmd} + r_{\text{pseudo}}|}{\left\{\tau_{r\max} + \left|(m_1 - m_2)uv - d_3 r + 2m_3\zeta k_r \overline{E}_r + m_3 k_r^2 \sin\left(\frac{\overline{E}_\psi}{2}\right)\right|\right\}} \tag{27b}$$

then (37) can be expressed as

$$\begin{aligned} v&=\overline{T}_u\left\{\cos\left((\psi_e)_{\text{pseudo}}\right)\overline{X}+\sin\left((\psi_e)_{\text{pseudo}}\right)\overline{Y}\right\}+T_u(E_u)\\ &=\left\{\cos\left((\psi_e)_{\text{pseudo}}\right)\overline{Y}-\sin\left((\psi_e)_{\text{pseudo}}\right)\overline{X}\right\}+T_u(E_u)\\ &=\left\{\sin(\theta)\cos\left((\psi_e)_{\text{pseudo}}\right)-\cos(\theta)\sin\left((\psi_e)_{\text{pseudo}}\right)\right\}\\ &\quad\cdot\sqrt{\overline{X}^2+\overline{Y}^2}+T_u(E_u)\\ &=-\sin\left((\psi_e)_{\text{pseudo}}-\theta\right)\sqrt{\overline{X}^2+\overline{Y}^2}+T_u(E_u)\\ &=v_{\text{pseudo}}+T_u(E_u). \end{aligned} \tag{39}$$

To show that $\overline{T}_u$ is a bounded function, we need to show that: 1) $T_u(E_u)$ is bounded and 2) $T_u(E_u)=0$ for $E_u=0$ [29]. First, as v is bounded from Lemma 1 and v_{pseudo} in (38) is also bounded, (30) shows that $T_u(E_u)$ is bounded. Second, the definition of $T_u(E_u)$ shows that $T_u(E_u)$ decreases to zero as E_u decreases to zero. Note that, when E_u and E_ψ are made to become zero, (30) shows that v becomes v_{pseudo}, and the right-hand side of (11b) becomes equal to zero. This is coherent to the fact that, even if u is zero, v-dynamics in the second row of (2) show the boundedness of v (i.e., that of $T_u(E_u)$). (Q.E.D.)

Based on Lemmas 1 and 2, the stability and performance of the above control system can be summarized as follows.

Theorem 1 (Tracking Control): Suppose that the Control Inputs $\tau=[\tau_u\ \tau_r]^T$ in (19), (21), (22), and (25), u_{pseudo} in (12), ψ_{pseudo} in (13), (17a) in the case of positive u_d (respectively, (13), (17b) in the case of negative u_d), and control gains k_p, $\overline{k}_p$, k_u, k_r, and k_ψ and filter time constants T_u, T_ψ, and T_r satisfying (15), (24), (27), and (40), shown at the bottom of the page, are used, where $\overline{T}_{u\max}$ in (34), $\overline{U}_{\zeta\max}$ in (A8a), and $\overline{U}_{E_u}$ in (A8b) are bounded. Then, the global ultimate boundedness of the position tracking errors (5) and yaw angle tracking error can be obtained and the ultimate bounds of the tracking errors can be adjusted by k_p, $\overline{k}_p$, k_u, k_r, k_ψ, T_u, T_ψ, and T_r and are dependent on $\overline{E}_\psi$, $\overline{U}_C$, and $\overline{R}_C$. Furthermore, the control inputs and velocities can be constrained as $|\tau_u|\le\tau_{u\max}$, $|\tau_r|\le\tau_{r\max}$, $|u|\le u_{\max}$, $|v|\le v_{\max}$, and $|r|\le r_{\max}$ for positive constants $v_{\max}$ and $r_{\max}$.

Proof: The first and second rows of (1) can be rearranged as

$$\begin{aligned} \dot{x}&=(u-u_{\text{pseudo}})\cos(\psi)+u_{\text{pseudo}}\cos(\psi)-v\sin(\psi)\\ &=E_u\cos(\psi)+u_{\text{pseudo}}\{\cos(\psi_d)\cos(\psi_e)-\sin(\psi_d)\sin(\psi_e)\}\\ &\quad-v_{\text{pseudo}}\{\sin(\psi_d)\cos(\psi_e)+\cos(\psi_d)\sin(\psi_e)\}\\ &\quad-T_u(E_u)\cdot\sin(\psi)\\ &=E_u\cos(\psi)+\cos(\psi_d)\{u_{\text{pseudo}}\cos(\psi_e)-v_{\text{pseudo}}\sin(\psi_e)\}\\ &\quad-\sin(\psi_d)\{u_{\text{pseudo}}\sin(\psi_e)+v_{\text{pseudo}}\cos(\psi_e)\}\\ &\quad-T_u(E_u)\cdot\sin(\psi) \end{aligned} \tag{41a}$$

$$\begin{aligned} \dot{y}&=(u-u_{\text{pseudo}})\sin(\psi)+u_{\text{pseudo}}\sin(\psi)+v\cos(\psi)\\ &=E_u\sin(\psi)+u_{\text{pseudo}}\{\sin(\psi_d)\cos(\psi_e)+\cos(\psi_d)\sin(\psi_e)\}\\ &\quad+v_{\text{pseudo}}\{\cos(\psi_d)\cos(\psi_e)-\sin(\psi_d)\sin(\psi_e)\}\\ &\quad+T_u(E_u)\cdot\cos(\psi)\\ &=E_u\sin(\psi)+\sin(\psi_d)\{u_{\text{pseudo}}\cos(\psi_e)-v_{\text{pseudo}}\sin(\psi_e)\}\\ &\quad+\cos(\psi_d)\{u_{\text{pseudo}}\sin(\psi_e)+v_{\text{pseudo}}\cos(\psi_e)\}\\ &\quad+T_u(E_u)\cdot\cos(\psi). \end{aligned} \tag{41b}$$

By substituting u_{pseudo} in (18) and v_{pseudo} in (38) into (41), we have

$$\begin{aligned} \dot{x}&=E_u\cos(\psi)\\ &\quad+\cos(\psi_d)\left\{\cos\left((\psi_e)_{\text{pseudo}}-\theta\right)\cos(\psi_e)\right.\\ &\qquad\left.+\sin\left((\psi_e)_{\text{pseudo}}-\theta\right)\sin(\psi_e)\right\}\\ &\quad\cdot\sqrt{\overline{X}^2+\overline{Y}^2}\\ &\quad-\sin(\psi_d)\left\{\cos\left((\psi_e)_{\text{pseudo}}-\theta\right)\sin(\psi_e)\right.\\ &\qquad\left.-\sin\left((\psi_e)_{\text{pseudo}}-\theta\right)\cos(\psi_e)\right\}\\ &\quad\cdot\sqrt{\overline{X}^2+\overline{Y}^2}-T_u(E_u)\cdot\sin(\psi)\\ &=E_u\cos(\psi)\\ &\quad+\{\cos(\psi_d)\cos(E_\psi+\theta)-\sin(\psi_d)\sin(E_\psi+\theta)\}\\ &\quad\cdot\sqrt{\overline{X}^2+\overline{Y}^2}-T_u(E_u)\cdot\sin(\psi)\\ &=E_u\cos(\psi)+\cos(\psi_d)\left\{\cos(E_\psi)\overline{X}-\sin(E_\psi)\overline{Y}\right\}\\ &\quad-\sin(\psi_d)\left\{\sin(E_\psi)\overline{X}+\cos(E_\psi)\overline{Y}\right\}-T_u(E_u)\cdot\sin(\psi)\\ &=E_u\cos(\psi)+\cos(\psi_d)\left\{\overline{X}-2\sin^2(E_\psi/2)\overline{X}\right.\\ &\qquad\left.-2\sin(E_\psi/2)\cos(E_\psi/2)\overline{Y}\right\}\\ &\quad-\sin(\psi_d)\left\{2\sin(E_\psi/2)\cos(E_\psi/2)\overline{X}+\overline{Y}\right.\\ &\qquad\left.-2\sin^2(E_\psi/2)\overline{Y}\right\}-T_u(E_u)\cdot\sin(\psi) \end{aligned}$$

$$\mathrm{H}=\begin{pmatrix} -k_p\overline{k}_p & 0 & \frac{\overline{k}_p(1+\overline{T}_{u\max})}{2} & 0 & 0 & \frac{\overline{k}_p(1+\overline{T}_{u\max})+\overline{U}_{\zeta\max}}{2} & 0\\ 0 & -k_p\overline{k}_p & \frac{\overline{k}_p(1+\overline{T}_{u\max})}{2} & 0 & 0 & \frac{\overline{k}_p(1+\overline{T}_{u\max})+\overline{U}_{\zeta\max}}{2} & 0\\ \frac{\overline{k}_p(1+\overline{T}_{u\max})}{2} & \frac{\overline{k}_p(1+\overline{T}_{u\max})}{2} & -k_u & 0 & 0 & \frac{\overline{U}_{E_u}}{2} & 0\\ 0 & 0 & 0 & -\frac{k_r^2k_\psi}{\pi^2} & 0 & 0 & \frac{k_r^2/\pi+k_\psi^2/4}{2}\\ 0 & 0 & 0 & 0 & -2\zeta k_r & 0 & \frac{k_\psi}{4}\\ \frac{\overline{k}_p(1+\overline{T}_{u\max})+\overline{U}_{\zeta\max}}{2} & \frac{\overline{k}_p(1+\overline{T}_{u\max})+\overline{U}_{\zeta\max}}{2} & \frac{\overline{U}_{E_u}}{2} & 0 & 0 & -\left(\frac{1}{T_u}-\overline{U}_{E_u}\right) & 0\\ 0 & 0 & 0 & \frac{k_r^2/\pi+k_\psi^2/4}{2} & \frac{k_\psi}{4} & 0 & -\left(\frac{1}{T_r}-\frac{k_\psi}{2}\right) \end{pmatrix}<0 \tag{40}$$

$$
\begin{aligned}
&= E_u\cos(\psi) + \cos(\psi_d)\overline{X} - \sin(\psi_d)\overline{Y} \\
&\quad + \left[\cos(\psi_d)\left\{-\sin(E_\psi/2)\overline{X} - \cos(E_\psi/2)\overline{Y}\right\}\right. \\
&\qquad \left. -\sin(\psi_d)\left\{\cos(E_\psi/2)\overline{X} - \sin(E_\psi/2)\overline{Y}\right\}\right] \\
&\quad \cdot 2\sin(E_\psi/2) - T_u(E_u)\cdot\sin(\psi) \\
&= E_u\cos(\psi) + \dot{x}_d - k_p\tanh(\overline{k}_p x_e) \\
&\quad + \left[\cos(\psi_d)\left\{-\sin(E_\psi/2)\overline{X} - \cos(E_\psi/2)\overline{Y}\right\}\right. \\
&\qquad \left. -\sin(\psi_d)\left\{\cos(E_\psi/2)\overline{X} - \sin(E_\psi/2)\overline{Y}\right\}\right] \\
&\quad \cdot 2\sin(E_\psi/2) - T_u(E_u)\cdot\sin(\psi) \qquad (42a) \\
\dot{y} &= E_u\sin(\psi) \\
&\quad + \sin(\psi_d)\left\{\cos\left((\psi_e)_{\text{pseudo}} - \theta\right)\cos(\psi_e)\right. \\
&\qquad \left. + \sin\left((\psi_e)_{\text{pseudo}} - \theta\right)\sin(\psi_e)\right\} \\
&\quad \cdot\sqrt{\overline{X}^2 + \overline{Y}^2} \\
&\quad + \cos(\psi_d)\left\{\cos\left((\psi_e)_{\text{pseudo}} - \theta\right)\sin(\psi_e)\right. \\
&\qquad \left. - \sin\left((\psi_e)_{\text{pseudo}} - \theta\right)\cos(\psi_e)\right\} \\
&\quad \cdot\sqrt{\overline{X}^2 + \overline{Y}^2} + T_u(E_u)\cdot\cos(\psi) \\
&= E_u\sin(\psi) \\
&\quad + \{\sin(\psi_d)\cos(E_\psi + \theta) + \cos(\psi_d)\sin(E_\psi + \theta)\} \\
&\quad \cdot\sqrt{\overline{X}^2 + \overline{Y}^2} + T_u(E_u)\cdot\cos(\psi) \\
&= E_u\sin(\psi) + \sin(\psi_d)\left\{\cos(E_\psi)\overline{X} - \sin(E_\psi)\overline{Y}\right\} \\
&\quad + \cos(\psi_d)\left\{\sin(E_\psi)\overline{X} + \cos(E_\psi)\overline{Y}\right\} + T_u(E_u) \\
&\quad \cdot\cos(\psi) \\
&= E_u\sin(\psi) + \sin(\psi_d)\left\{\overline{X} - 2\sin^2(E_\psi/2)\overline{X}\right. \\
&\qquad \left. -2\sin(E_\psi/2)\cos(E_\psi/2)\overline{Y}\right\} \\
&\quad + \cos(\psi_d)\left\{2\sin(E_\psi/2)\cos(E_\psi/2)\overline{X} + \overline{Y}\right. \\
&\qquad \left. -2\sin^2(E_\psi/2)\overline{Y}\right\} + T_u(E_u)\cdot\cos(\psi) \\
&= E_u\sin(\psi) + \sin(\psi_d)\overline{X} + \cos(\psi_d)\overline{Y} \\
&\quad + \left[\sin(\psi_d)\left\{-\sin(E_\psi/2)\overline{X} - \cos(E_\psi/2)\overline{Y}\right\}\right. \\
&\qquad \left. + \cos(\psi_d)\left\{\cos(E_\psi/2)\overline{X} - \sin(E_\psi/2)\overline{Y}\right\}\right] \\
&\quad \cdot 2\sin(E_\psi/2) + T_u(E_u)\cdot\cos(\psi) \\
&= E_u\sin(\psi) + \dot{y}_d - k_p\tanh(\overline{k}_p y_e) \\
&\quad + \left[\sin(\psi_d)\left\{-\sin(E_\psi/2)\overline{X} - \cos(E_\psi/2)\overline{Y}\right\}\right. \\
&\qquad \left. + \cos(\psi_d)\left\{\cos(E_\psi/2)\overline{X} - \sin(E_\psi/2)\overline{Y}\right\}\right] \\
&\quad \cdot 2\sin(E_\psi/2) + T_u(E_u)\cdot\cos(\psi) \qquad (42b)
\end{aligned}
$$

where each of the last equalities follows by using $\overline{X}$ and $\overline{Y}$ in (9a) and (9b). Then, (42) can be combined as

$$
\begin{aligned}
\begin{pmatrix}\dot{x}_e \\ \dot{y}_e\end{pmatrix} &= \begin{pmatrix}-k_p\tanh(\overline{k}_p x_e) \\ -k_p\tanh(\overline{k}_p y_e)\end{pmatrix} + \begin{pmatrix}\cos(\psi) & -\sin(\psi) \\ \sin(\psi) & \cos(\psi)\end{pmatrix} \\
&\quad \times \begin{pmatrix}E_u \\ T_u(E_u)\end{pmatrix} + \begin{pmatrix}\cos(\psi_d) & -\sin(\psi_d) \\ \sin(\psi_d) & \cos(\psi_d)\end{pmatrix} \\
&\quad \times \begin{pmatrix}-\sin(E_\psi/2) & -\cos(E_\psi/2) \\ \cos(E_\psi/2) & -\sin(E_\psi/2)\end{pmatrix}\begin{pmatrix}\overline{X} \\ \overline{Y}\end{pmatrix} \\
&\quad \cdot 2\sin(E_\psi/2). \qquad (43)
\end{aligned}
$$

Here, we introduce

$$
\begin{aligned}
y_u &= u_{cmd} - u_{\text{pseudo}} (= E_u - \overline{E}_u) && (44a)\\
y_\psi &= \psi_{cmd} - \psi_{\text{pseudo}} (= E_\psi - \overline{E}_\psi) && (44b)\\
y_r &= r_{cmd} - r_{\text{pseudo}} (= E_r - \overline{E}_r). && (44c)
\end{aligned}
$$

Then, $T_u(E_u)$ in (32) can be expressed as

$$
T_u(E_u) = \overline{T}_u(\overline{E}_u + y_u). \qquad (45)
$$

Thus, using $E_u = \overline{E}_u + y_u$ and from (44a), (43) becomes

$$
\begin{aligned}
\begin{pmatrix}\dot{x}_e \\ \dot{y}_e\end{pmatrix} &= \begin{pmatrix}-k_p\tanh(\overline{k}_p x_e) \\ -k_p\tanh(\overline{k}_p y_e)\end{pmatrix} + \begin{pmatrix}A_{11} & A_{12} \\ A_{21} & A_{22}\end{pmatrix}\begin{pmatrix}\overline{E}_u \\ y_u\end{pmatrix} \\
&\quad + \begin{pmatrix}\cos(\psi_d) & -\sin(\psi_d) \\ \sin(\psi_d) & \cos(\psi_d)\end{pmatrix} \\
&\quad \times \begin{pmatrix}-\sin(E_\psi/2) & -\cos(E_\psi/2) \\ \cos(E_\psi/2) & -\sin(E_\psi/2)\end{pmatrix}\begin{pmatrix}\overline{X} \\ \overline{Y}\end{pmatrix} \\
&\quad \cdot 2\sin(E_\psi/2) \qquad (46)
\end{aligned}
$$

where
$\begin{pmatrix}A_{11} & A_{12} \\ A_{21} & A_{22}\end{pmatrix} := \begin{pmatrix}\cos(\psi) - \sin(\psi)\overline{T}_u & \cos(\psi) - \sin(\psi)\overline{T}_u \\ \sin(\psi) + \cos(\psi)\overline{T}_u & \sin(\psi) + \cos(\psi)\overline{T}_u\end{pmatrix}$
is bounded by $\begin{pmatrix}1 & 1 \\ 1 & 1\end{pmatrix}(1 + \overline{T}_{u\max})$ from (34). Thus, it is sufficient to make $\overline{E}_u$, y_u, and E_ψ remain in a small neighborhood of zero.

Now, we choose the Lyapunov function candidate as $V_s = V_p + V_u + V_\psi + V_r$, where $V_p = \ln\{\cosh(\overline{k}_p x_e)\} + \ln\{\cosh(\overline{k}_p y_e)\}$, $V_u = (1/2)\overline{E}_u^2$, $V_\psi = 2k_r^2\{1 - \cos(\overline{E}_\psi/2)\}$, $V_r = (1/2)\overline{E}_r^2$, and $\zeta := [\zeta_1, \zeta_2]^T = [\tanh(\overline{k}_p x_e), \tanh(\overline{k}_p y_e)]^T$ which satisfies $|\zeta_1|, |\zeta_2| \le 1$. Then, (46) and (28) give

$$
\begin{aligned}
\dot{V}_s &\le -k_p\overline{k}_p\zeta^T\zeta + \overline{k}_p\zeta^T\begin{pmatrix}A_{11} & A_{12} \\ A_{21} & A_{22}\end{pmatrix}\begin{pmatrix}\overline{E}_u \\ y_u\end{pmatrix} \\
&\quad + \overline{k}_p|\zeta_1\overline{X} + \zeta_2\overline{Y}|\cdot 2\,|\sin(E_\psi/2)| \\
&\quad - k_u\overline{E}_u^2 + k_r^2\sin(\overline{E}_\psi/2)\left\{-k_\psi\sin(\overline{E}_\psi/2) + E_r\right\} \\
&\quad + \overline{E}_r\left\{-2\zeta k_r\overline{E}_r - k_r^2\sin(\overline{E}_\psi/2)\right\} \\
&\le -k_p\overline{k}_p\zeta^T\zeta - k_u\overline{E}_u^2 - k_r^2 k_\psi\sin^2(\overline{E}_\psi/2) - 2\zeta k_r\overline{E}_r^2 \\
&\quad + \overline{k}_p\overline{E}_u\{A_{11}\zeta_1 + A_{21}\zeta_2\} + \overline{k}_p y_u\{A_{12}\zeta_1 + A_{22}\zeta_2\} \\
&\quad + \left(2\overline{k}_p\sqrt{2(\overline{X}^2 + \overline{Y}^2)} + k_r^2|y_r|\right)\cdot\left|\sin(\overline{E}_\psi/2)\right| \\
&\le -k_p\overline{k}_p\zeta^T\zeta - k_u\overline{E}_u^2 - \left(k_r^2 k_\psi/\pi^2\right)\overline{E}_\psi^2 - 2\zeta k_r\overline{E}_r^2 \\
&\quad + \overline{k}_p\left(|\overline{E}_u| + |y_u|\right)\cdot(|\zeta_1| + |\zeta_2|)\cdot(1 + \overline{T}_{u\max}) \\
&\quad + \left(2\overline{k}_p\sqrt{2(\overline{X}^2 + \overline{Y}^2)} + k_r^2|y_r|\right)\cdot|\overline{E}_\psi|/\pi \qquad (47)
\end{aligned}
$$

where inequalities are obtained by using Cauchy–Schwarz inequality and (34).

Considering that y_u and y_r need to be reduced in (47), we also choose the Lyapunov function candidate $V_y = V_{yu} + V_{yr}$

TABLE I
INITIAL CONDITIONS ON VELOCITIES AND POSTURE (POSITION AND YAW ANGLE) OF REFERENCE AND UNDERACTUATED SHIP

	Reference velocities		Reference initial posture ($[x_d(0), y_d(0), \psi_d(0)]$) (m, m, rad)	Ship initial posture ($[x(0), y(0), \psi(0)]$) (m, m, rad)
	$u_d(m/\text{sec})$	$r_d(rad/\text{sec})$		
Scenario 1	1	$0,\ 0 \le t < 50$ $0.1,\ 50 \le t \le 100$	[0.5, 0.5, 0.2]	[15, 15, 0.7]
Scenario 2	-1	$0.1\sin(0.04\pi t)$	$[0, 0, 7/4\pi]$	$[17, 4, \pi]$
Scenario 3	10	$0,\ 0 \le t < 65$ $0.05,\ 65 \le t \le 100$	[0, 0, 0]	[-10, 10, 0.1]

where $V_{yu} = (1/2)y_u^2$, $V_{yr} = (1/2)y_r^2$. To obtain their time derivatives, we first obtain

$$\dot{y}_u = -y_u/T_u - \dot{u}_{\text{pseudo}} \tag{48a}$$
$$\dot{y}_r = -y_r/T_r - \dot{r}_{\text{pseudo}} \tag{48b}$$

by using (44) and (21). Thus, using (A6) and (A9), we have

$$y_u\dot{y}_u \le -y_u^2/T_u + |y_u| \cdot \left|\overline{U}_{\zeta_1}\zeta_1 + \overline{U}_{\zeta_2}\zeta_2 + \overline{U}_{\overline{E}_u}\overline{E}_u + \overline{U}_{y_u}y_u + \overline{U}_C\right| \tag{49a}$$
$$y_r\dot{y}_r \le -y_r^2/T_r + |y_r| \cdot \left|\overline{R}_{\overline{E}_\psi}\overline{E}_\psi + \overline{R}_{\overline{E}_r}\overline{E}_r + \overline{R}_{y_r}y_r + \overline{R}_C\right| \tag{49b}$$

where the detailed notation can be referred to Appendix A. Also, it follows that

$$\begin{aligned}\dot{V}_y \le & -y_u^2/T_u - y_r^2/T_r + |y_u| \cdot \left|\overline{U}_{\zeta_1}\zeta_1 + \overline{U}_{\zeta_2}\zeta_2 + \overline{U}_{\overline{E}_u}\overline{E}_u + \overline{U}_{y_u}y_u + \overline{U}_C\right| \\ & + |y_r| \cdot \left|\overline{R}_{\overline{E}_\psi}\overline{E}_\psi + \overline{R}_{\overline{E}_r}\overline{E}_r + \overline{R}_{y_r}y_r + \overline{R}_C\right| \\ \le & -\left(1/T_u - \overline{U}_{E_u}\right)y_u^2 - \left\{1/T_r - (k_\psi/2)\right\}y_r^2 \\ & + |y_u|\left\{\overline{U}_{\zeta\max} \cdot (|\zeta_1| + |\zeta_2|) + \overline{U}_{E_u} \cdot |\overline{E}_u| + |\overline{U}_C|\right\} \\ & + |y_r|\left\{\left(k_\psi^2/4\right)|\overline{E}_\psi| + (k_\psi/2)|\overline{E}_r| + |\overline{R}_C|\right\}\end{aligned} \tag{50}$$

where the second inequality is obtained by using (A8) and (A11).

If we choose the Lyapunov function candidate as $V_T = V_s + V_y$, then its time derivative can be obtained by using (47) and (50) as

$$\begin{aligned}\dot{V}_T \le & -k_p\overline{k}_p\zeta^T\zeta - k_u\overline{E}_u^2 - \left(k_r^2k_\psi/\pi^2\right)\overline{E}_\psi^2 - 2\zeta k_r\overline{E}_r^2 \\ & - \left(1/T_u - \overline{U}_{E_u}\right)y_u^2 - \left\{1/T_r - (k_\psi/2)\right\}y_r^2 \\ & + \overline{k}_p\left(|\overline{E}_u| + |y_u|\right) \cdot (|\zeta_1| + |\zeta_2|) \cdot (1 + \overline{T}_{u\max}) \\ & + 2\overline{k}_p\sqrt{2(\overline{X}^2 + \overline{Y}^2)} \cdot |\overline{E}_\psi|/\pi \\ & + |y_u|\left\{\overline{U}_{\zeta\max} \cdot (|\zeta_1| + |\zeta_2|) + \overline{U}_{E_u} \cdot |\overline{E}_u| + |\overline{U}_C|\right\} \\ & + |y_r|\left\{\left(k_r^2/\pi + k_\psi^2/4\right) \cdot |\overline{E}_\psi| + (k_\psi/2)|\overline{E}_r| + |\overline{R}_C|\right\} \\ \le & \,\Xi^T\mathrm{H}\Xi + 2\overline{k}_p\sqrt{2(\overline{X}^2 + \overline{Y}^2)} \cdot |\overline{E}_\psi|/\pi + |y_u| \cdot |\overline{U}_C| \\ & + |y_r| \cdot |\overline{R}_C|\end{aligned} \tag{51}$$

where $\Xi = (|\zeta_1|\ |\zeta_2|\ |\overline{E}_u|\ |\overline{E}_\psi|\ |\overline{E}_r|\ |y_u|\ |y_r|)^T$. Since H is negative definite from (40), and $\overline{E}_\psi$, $\overline{U}_C$ and $\overline{R}_C$ are bounded, the global ultimate boundedness of the tracking errors can be guaranteed. In other words, since the boundedness of the $\overline{E}_\psi$, $\overline{U}_C$, and $\overline{R}_C$ is shown, it can be proved that the global ultimate boundedness of the tracking errors can be achieved instead of the semi-global one, which is usual in the case of DSC method. In particular, the ultimate bound is dependent on the values of $\overline{E}_\psi, \overline{U}_C$ (i.e., $(\dot{\psi}_e)_{\text{pseudo}}$ as in (A2), and E_ψ as in (A7)), and $\overline{R}_C$ (i.e., $\dot{\psi}_{\text{pseudo}}$ as in (A10)), and it can be adjusted by making the real parts of the eigenvalues of H much more negative through the proper choice of k_u, k_r, k_ψ, T_u, T_ψ, and T_r. It should be noted here that sufficiently large k_u, k_ψ, and k_r which are high gains of u-, ψ-, and r-systems can be expected to imply the asymptotic convergence of u, ψ, and r to u_{pseudo}, ψ_{pseudo}, and ψ_{pseudo}, but the size of the region of attraction can be reduced and even instability can happen as noticed in [28]. This completes the proof for the global tracking control of underactuated ships using dynamic surface control. (Q.E.D.)

Remark 4: The proposed method is beneficial in that, due to the modular structure, various kinds of controller can be employed as a controller for the dynamic part. For example, the controller in (25) can be simplified such as $\overline{\tau}_u = -k_uE_u$, $\overline{\tau}_r = -2\zeta k_rE_r - k_r^2\sin(E_\psi/2)$), in which case it is possible to have almost the same performance as those in the next section, and the stability analysis can be done in the same way.

IV. SIMULATION RESULTS

Simulation results of the proposed method for the underactuated ship are presented in this section. The parameters of the kinematics equation (1) and dynamics equation (2) are $m_1 = 120 \times 10^3$ kg, $m_2 = 172.9 \times 10^3$ kg, $m_3 = 636 \times 10^5$ kg $\cdot$ m^2, $d_1 = 215 \times 10^2$ kg $\cdot$ s^{-1}, $d_2 = 97 \times 10^3$ kg $\cdot$ s^{-1}, $d_3 = 802 \times 10^4$ kg $\cdot$ m^2 $\cdot$ s^{-1} as in [20]. The controller is given by (12), (13), (17), (19), (21), (22), and (25). The reference trajectory is generated using the reference model in (3) and (4), where the desired sway velocity is fixed as $v_d = 0$ such that more general trajectories are generated. Initial position and yaw angle tracking errors are assumed to exist in several scenarios as shown in Table I, and initial velocities are $(u(0), v(0), r(0)) = (0, 0, 0)$. Here, the reference trajectories of scenarios 1 and 2 are: 1) a straight line combined with the circle in forward direction and 2) sinusoidal curve in backward direction. Considering that the minimum turning radius of the ship is 155 m in [21], the scenario 1 in [18] and

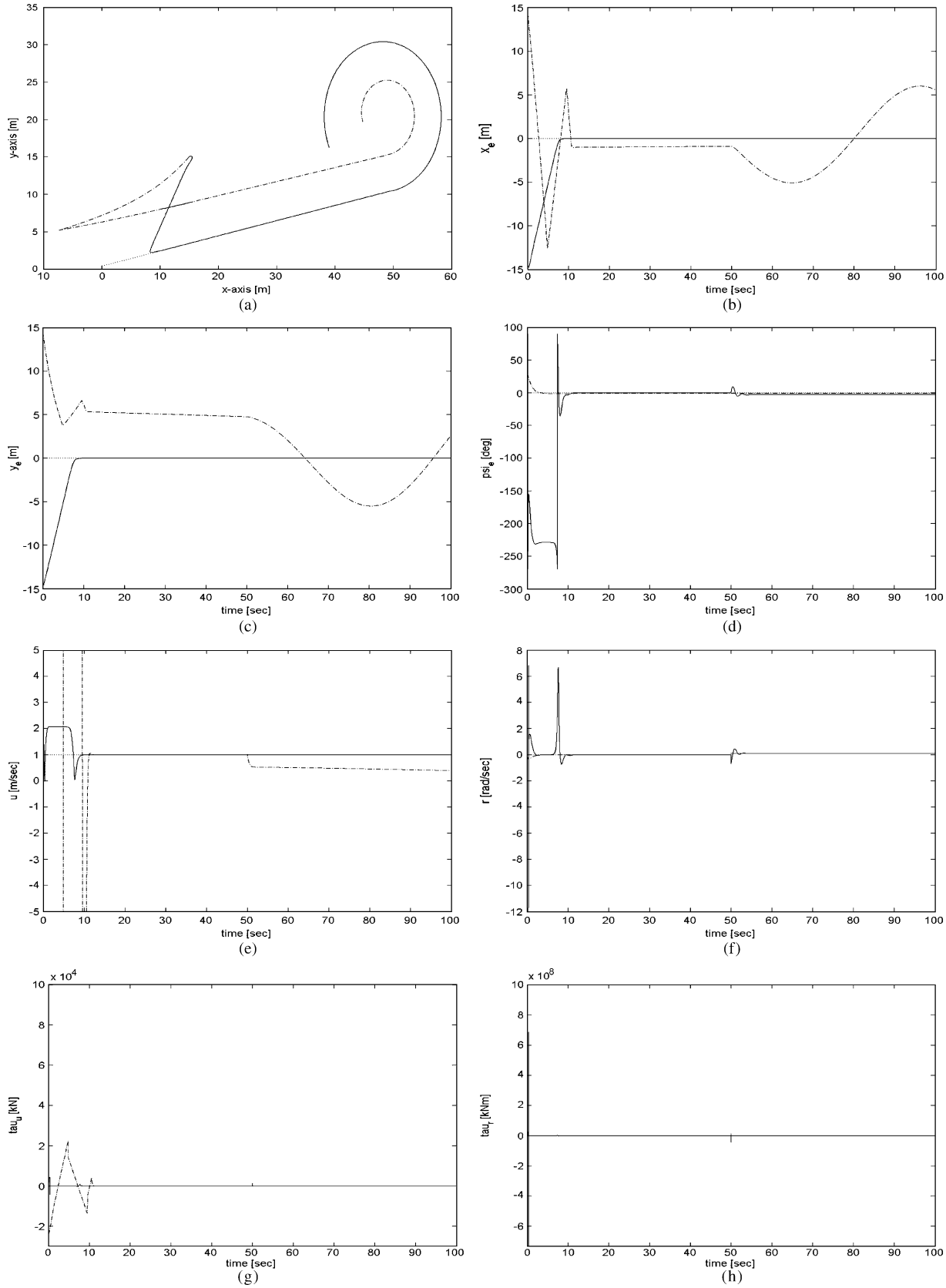

Fig. 3. Tracking performance under constraints (Scenario 1) (dotted line: reference; solid line: proposed method; dashed–dotted line: previous method [20]). (a) $x - y$ plot, (b) tracking error (x_e), (c) tracking error (y_e), (d) tracking error (ψ_e), (e) forward velocity u, (f) yaw velocity r, (g) control input τ_u, and (h) control input τ_r.

the scenario 2 in [5] do require much larger yaw velocity r than scenario 3, in which case the reference trajectory is a straight line followed by a circle with a radius of 200 m. Accordingly, to demonstrate the performance of the proposed method,

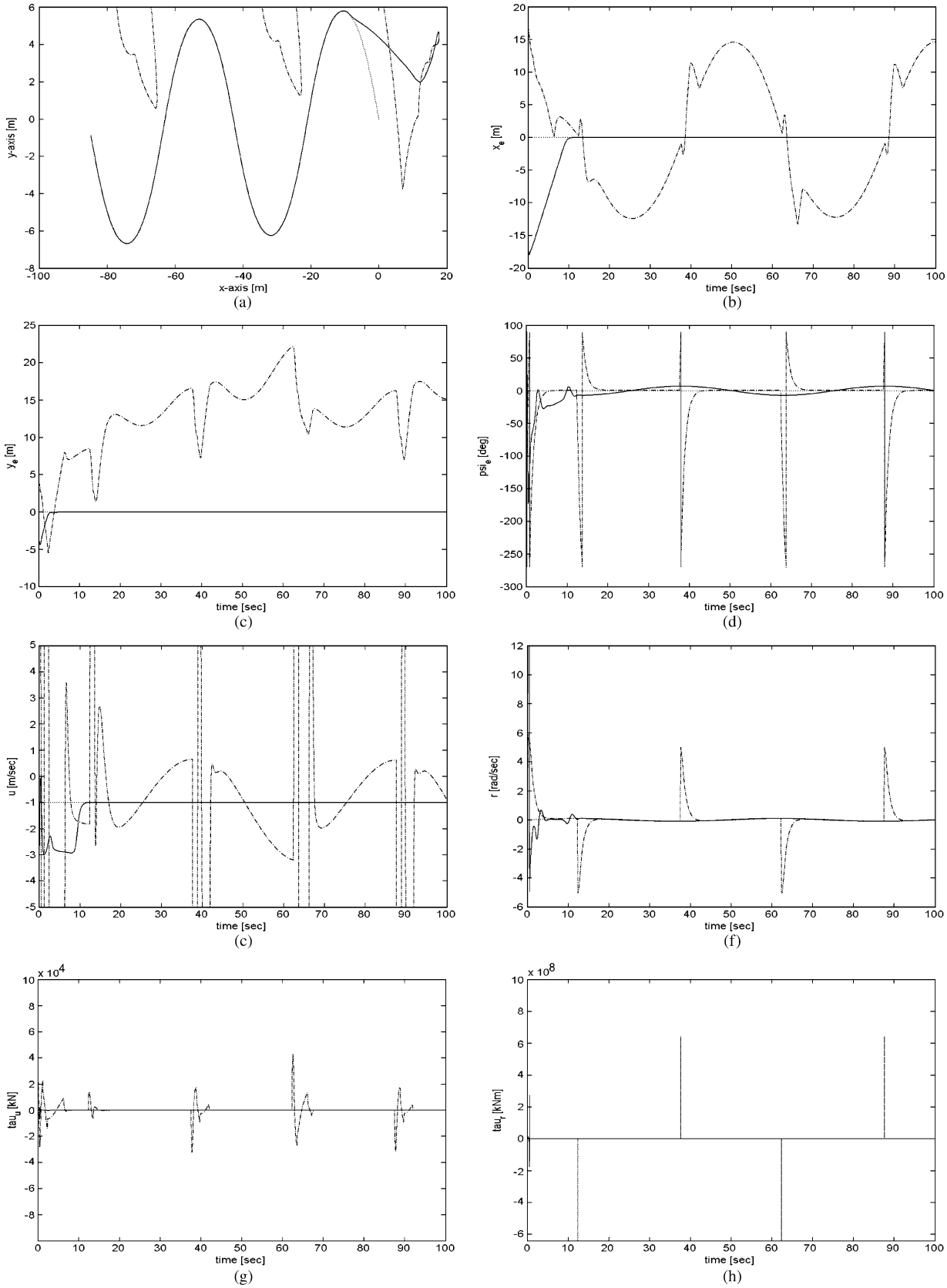

Fig. 4. Tracking performance under constraints (Scenario 2) (dotted line: reference; solid line: proposed method; dashed-dotted line: previous method [20]). (a) $x-y$ plot, (b) tracking error (x_e), (c) tracking error (y_e), (d) tracking error (ψ_e),(e) forward velocity u, (f) yaw velocity r, (g) control input τ_u, and (h) control input τ_r.

whereas the input constraints are included as $\tau_{u\max} = 10^5$ kN, $\tau_{r\max} = 10^9$ kN $\cdot$ m for all scenarios, the velocity constraints are included as $u_{\max} = 5$ m/s, $r_{\max} = 12$ rad/s in the case of scenarios 1 and 2, and $u_{\max} = 20$ m/s, $r_{\max} = 2$ rad/s in the

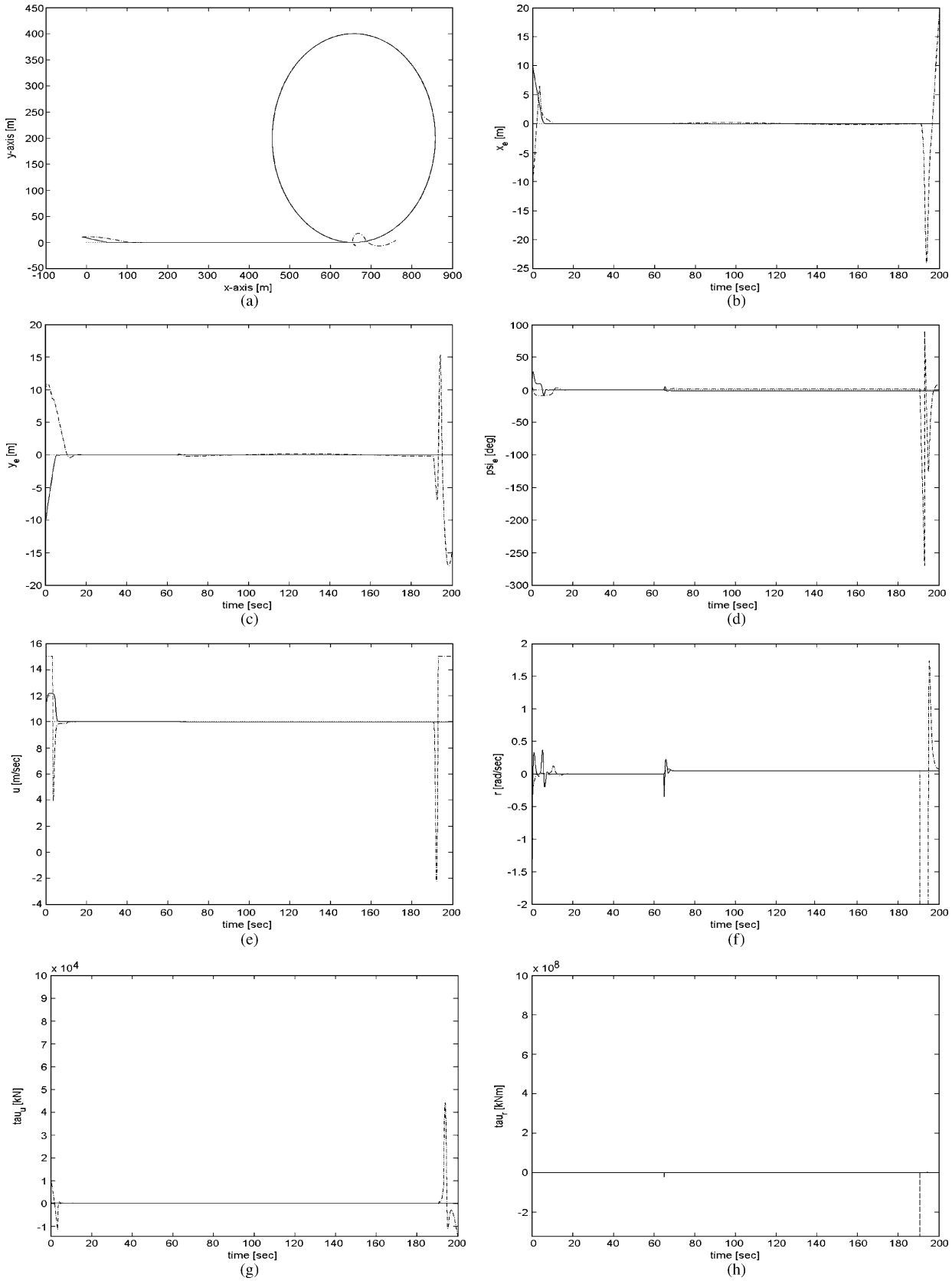

Fig. 5. Tracking performance under constraints (Scenario 3) (dotted line: reference; solid line: proposed method; dashed–dotted line: previous method [20]). (a) $x-y$ plot, (b) tracking error (x_e), (c) tracking error (y_e), (d) tracking error (ψ_e),(e) forward velocity u, (f) yaw velocity r, (g) control input τ_u, and (h) control input τ_r.

case of scenario 3. To satisfy the conditions (24) and (27) in addition to (15) and (40) in Theorem 1, the design parameters of the controller are chosen as $k_p = 2$, $\overline{k}_p = 1$, $\zeta = 0.9$, $k_u = 100$, $k_\psi = 2$, $k_r = 20$, $T_u = 0.0005$, $T_\psi = 0.1$, and

$T_r = 0.001$ in the case of scenarios 1 and 2, which can be easily done by using the MATLAB commands by trial and error. On the other hand, in the case of scenario 3, the design parameters k_ψ and T_u are adjusted to 0.5 and 0.005, respectively. It should be noted that T_u, T_ψ, and T_r are obtained from the conditions in (27a), (24b), and (27b), respectively. In order to verify the robustness of the proposed controller, the disturbances in [20] which act on the surge, sway, and yaw dynamics are chosen as $\tau_{wu}(t) = 0.1\ m_1\ \mathrm{rand}(\cdot)$, $\tau_{wv}(t) = 0.1\ m_2\ \mathrm{rand}(\cdot)$, $\tau_{wr}(t) = 0.1\ m_3\ \mathrm{rand}(\cdot)$ where $\mathrm{rand}(\cdot)$ is Gaussian random noise with mean 0 and variance 1. It will be shown below that even with these disturbances, satisfactory performance could be maintained, thus showing the robustness of the hierarchical proposed controller, as commented in [26]. In particular, the previous method in [20] is compared with the proposed method, under the same aforementioned conditions.

Fig. 3 shows the results for tracking the straight line combined with the circle. The position and yaw angle tracking errors in Fig. 3(a)–(c) are sufficiently small even with the input and velocity constraints in the case of the proposed method, and tracking performance is relatively faster when compared with the controller in [20]. It is noted that the previous method [20] can show the good performance when the input and velocity constraints do not exist, but it results in the significantly degraded performance in the presence of those constraints. As for the performance of the proposed method, we need to include the following remarks. ψ_e in Fig. 3(d) converges to zero when tracking the straight line as ψ_{pseudo} becomes constant. Then, ψ_e remains bounded when tracking the circle as ψ_{pseudo} is time-varying. As stated in the proof of Theorem 1, the ultimate bounds of the position and yaw angle tracking errors are dependent on $\overline{E}_\psi$, E_ψ, $(\dot{\psi}_e)_{\mathrm{pseudo}}$, $\dot{\psi}_{\mathrm{pseudo}}$. Among them, $\dot{\psi}_{\mathrm{pseudo}}$ and $(\dot{\psi}_e)_{\mathrm{pseudo}}$ are more influential to the magnitude of ultimate bounds than other terms, which are therefore dependent on the magnitude of the curvature of the reference trajectory and the time-varying ψ_{pseudo} (or the reference yaw velocity). This is also noticed in [23], where the orientation error cannot tend to zero in the case of nonzero lateral velocity, especially when the curvature of the reference trajectory changes. Even though the yaw angle tracking error in Fig. 3(d) does not converge to zero, position tracking errors in Fig. 3(a) and (b) remain sufficiently small and the surge direction is retained in the desired forward direction by generating ψ_{pseudo} as (17a) or (17b). As observed in [16], the reason for state-tracking rather than output-tracking is to inhibit the ship from turning around and following the reference trajectory backward, which does not happen in our result. Fig. 3(e) and (f) shows that actual forward velocity and yaw velocity follow their reference values.

Fig. 4 shows the results for Scenario 2. In this figure, we can see that a sinusoidal trajectory with the time varying velocity can be followed by the proposed method as position tracking errors approach zero. We can see in Fig. 4(a) that, in the case of the proposed method, the ship follows the path of the reference trajectory in the backward direction and the position tracking error remains almost zero, but the yaw angle tracking error remains different from 0° in Fig. 4(d) due to the rapidly changing curvature. However, the previous method [20] cannot achieve the tracking performance at all. It should be noted here that this reference trajectory is selected for wheeled mobile robots in [5], which can be much difficult to follow for the underactuated ships. As ψ_{pseudo} is generated as (13) and (17a) or (17b), depending on the forward or backward direction, the tracking of the straight line could be achieved even with the large initial yaw angle tracking error. This is possible since our scheme can be applied for a whole range of the yaw angle tracking error ($\psi_e(0) > 0.5\pi$ in the case of Scenario 3), in contrast to [21] which requires the yaw angle tracking error to satisfy $|\psi_e(0)| < 0.5\pi$.

In Fig. 5, the tracking performance of the straight line followed by a circle with a radius of 200 m is shown. In this case, the proposed method shows somewhat faster transient response, compared with the previous method [20]. In particular, the previous method shows deteriorated response when the yaw angle becomes numerically discontinuous due to the difference between 0° and 360°, which does not happen in the proposed method as stated in *Remark 3*.

In all of the above results, the actual velocity u and r converges to u_d and r_d, respectively, and the validity of the proposed method is demonstrated. In particular, the sign of the actual forward velocity is always maintained as that of reference forward velocity, as can be seen in Figs. 3(e), 4(e), and 5(e). As the constraints on inputs and velocities can be different depending on the type of each ship, the reference trajectory should be chosen to be a feasible trajectory for the ship to follow under the input and velocity constraints, which is another issue and can be solved through the motion planning problem or through the path-following problem.

V. CONCLUSION

Unlike the numerous previous approaches adopting the modular structure, which usually involves the restrictions on either the initial conditions or the yaw motion, the proposed method using dynamic surface control method involves the stability analysis of the overall kinematics and dynamics rigorously as in the backstepping method to guarantee the global uniform ultimate boundedness of the tracking errors in both position and yaw angle even in the presence of the input and velocity constraints. In particular, we could avoid the complex control structure, which is common in the backstepping technique due to the explosion of derivative terms of the states, such that the other various types of dynamic controllers can be easily employed along with the proposed kinematic controllers in the practical applications. Since the proposed control law does not require the reference yaw velocity to be persistently exciting nor the initial yaw angle to be restricted, more general types of reference trajectories such as sinusoidal curves, circles, and straight lines can be followed, as demonstrated in the numerical simulations. Furthermore, the gains in the choice of control inputs, pseudo forward velocity, and pseudo yaw angle can be adjusted to satisfy the input and velocity constraints. The issues on the controller state observation are also important problems for practical implementation which need to be investigated in future studies.

APPENDIX A
DERIVATION OF (49)

From (12), (9a), and (9b), we can obtain

$$\begin{aligned}\dot{u}_{\text{pseudo}} =& -\sin\left((\psi_e)_{\text{pseudo}}\right)(\dot{\psi}_e)_{\text{pseudo}}\overline{X}\\ &+\cos\left((\psi_e)_{\text{pseudo}}\right)\dot{\overline{X}}\\ &+\cos\left((\psi_e)_{\text{pseudo}}\right)(\dot{\psi}_e)_{\text{pseudo}}\overline{Y}\\ &+\sin\left((\psi_e)_{\text{pseudo}}\right)\dot{\overline{Y}}\\ =& -\sin\left((\psi_e)_{\text{pseudo}}\right)(\dot{\psi}_e)_{\text{pseudo}}\\ &\times\{u_d-\cos(\psi_d)k_p\zeta_1-\sin(\psi_d)k_p\zeta_2\}\\ &+\cos\left((\psi_e)_{\text{pseudo}}\right)\\ &\times\Big\{\dot{u}_d+\sin(\psi_d)\dot{\psi}_d k_p\zeta_1-\cos(\psi_d)k_p\dot{\zeta}_1\\ &\quad-\cos(\psi_d)\dot{\psi}_d k_p\zeta_2-\sin(\psi_d)k_p\dot{\zeta}_2\Big\}\\ &+\cos\left((\psi_e)_{\text{pseudo}}\right)(\dot{\psi}_e)_{\text{pseudo}}\\ &\times\{v_d+\sin(\psi_d)k_p\zeta_1-\cos(\psi_d)k_p\zeta_2\}\\ &+\sin\left((\psi_e)_{\text{pseudo}}\right)\\ &\times\Big\{\dot{v}_d+\cos(\psi_d)\dot{\psi}_d k_p\zeta_1+\sin(\psi_d)k_p\dot{\zeta}_1\\ &\quad+\sin(\psi_d)\dot{\psi}_d k_p\zeta_2-\cos(\psi_d)k_p\dot{\zeta}_2\Big\}\\ \le&\left|(\dot{\psi}_e)_{\text{pseudo}}\left\{|u_d|+\sqrt{2}k_p\right\}\right|+|\dot{u}_d|\\ &+\cos\left((\psi_e)_{\text{pseudo}}\right)\\ &\times\Big\{\sin(\psi_d)\dot{\psi}_d k_p\zeta_1-\cos(\psi_d)k_p\dot{\zeta}_1\\ &\quad-\cos(\psi_d)\dot{\psi}_d k_p\zeta_2-\sin(\psi_d)k_p\dot{\zeta}_2\Big\}\\ &+\left|(\dot{\psi}_e)_{\text{pseudo}}\left\{|v_d|+\sqrt{2}k_p\right\}\right|+|\dot{v}_d|\\ &+\sin\left((\psi_e)_{\text{pseudo}}\right)\\ &\times\Big\{\cos(\psi_d)\dot{\psi}_d k_p\zeta_1+\sin(\psi_d)k_p\dot{\zeta}_1\\ &\quad+\sin(\psi_d)\dot{\psi}_d k_p\zeta_2-\cos(\psi_d)k_p\dot{\zeta}_2\Big\}\\ =&U_{\zeta_1}\zeta_1+U_{\zeta_2}\zeta_2+U_{\dot{\zeta}_1}\dot{\zeta}_1+U_{\dot{\zeta}_2}\dot{\zeta}_2+U_C \qquad \text{(A1)}\end{aligned}$$

where

$$\begin{aligned}U_{\zeta_1} =& \cos\left((\psi_e)_{\text{pseudo}}\right)\sin(\psi_d)\dot{\psi}_d k_p\\ &+\sin\left((\psi_e)_{\text{pseudo}}\right)\cos(\psi_d)\dot{\psi}_d k_p\\ =&\sin(\psi_{\text{pseudo}})r_d k_p\\ U_{\zeta_2} =& -\cos\left((\psi_e)_{\text{pseudo}}\right)\cos(\psi_d)\dot{\psi}_d k_p\\ &+\sin\left((\psi_e)_{\text{pseudo}}\right)\sin(\psi_d)\dot{\psi}_d k_p\\ =&-\cos(\psi_{\text{pseudo}})r_d k_p\\ U_{\dot{\zeta}_1} =& -\cos\left((\psi_e)_{\text{pseudo}}\right)\cos(\psi_d)k_p\\ &+\sin\left((\psi_e)_{\text{pseudo}}\right)\sin(\psi_d)k_p\\ =&-\cos(\psi_{\text{pseudo}})k_p\\ U_{\dot{\zeta}_2} =& -\cos\left((\psi_e)_{\text{pseudo}}\right)\sin(\psi_d)k_p\\ &-\sin\left((\psi_e)_{\text{pseudo}}\right)\cos(\psi_d)k_p\\ =&-\sin(\psi_{\text{pseudo}})k_p\\ U_C =& \left|(\dot{\psi}_e)_{\text{pseudo}}\left\{|u_d|+\sqrt{2}k_p\right\}\right|\\ &+\left|(\dot{\psi}_e)_{\text{pseudo}}\left\{|v_d|+\sqrt{2}k_p\right\}\right|\\ &+|\dot{u}_d|+|\dot{v}_d| \qquad \text{(A2)}\end{aligned}$$

are all bounded and the upper bounds are given by

$$|U_{\zeta_1}|,\ |U_{\zeta_2}|\le k_p r_{\max},\quad \left|U_{\dot{\zeta}_1}\right|,\ \left|U_{\dot{\zeta}_2}\right|\le k_p. \qquad \text{(A3)}$$

Note that the boundedness of $\dot{\psi}_{\text{pseudo}}$ (or $(\dot{\psi}_e)_{\text{pseudo}}$) can be inferred from the fact that (21b) gives

$$\dot{y}_\psi = -\sin(y_\psi)/T_\psi+\dot{\psi}_{\text{pseudo}} \qquad \text{(A4)}$$

and the definition of y_ψ readily shows its boundedness. Also, (46) gives

$$\begin{aligned}\begin{pmatrix}\dot{\zeta}_1\\ \dot{\zeta}_2\end{pmatrix} =& \begin{pmatrix}-k_p\overline{k}_p\text{sech}(\overline{k}_p x_e)\zeta_1\\ -k_p\overline{k}_p\text{sech}(\overline{k}_p y_e)\zeta_2\end{pmatrix}+\begin{pmatrix}\overline{A}_{11} & \overline{A}_{12}\\ \overline{A}_{21} & \overline{A}_{22}\end{pmatrix}\begin{pmatrix}\overline{E}_u\\ y_u\end{pmatrix}\\ &+\begin{pmatrix}\cos(\psi_d) & -\sin(\psi_d)\\ \sin(\psi_d) & \cos(\psi_d)\end{pmatrix}\\ &\times\begin{pmatrix}-\sin(E_\psi/2) & -\cos(E_\psi/2)\\ \cos(E_\psi/2) & -\sin(E_\psi/2)\end{pmatrix}\\ &\cdot\begin{pmatrix}\overline{k}_p\text{sech}(\overline{k}_p x_e)\overline{X}\\ \overline{k}_p\text{sech}(\overline{k}_p y_e)\overline{Y}\end{pmatrix}\cdot 2\sin(E_\psi/2) \qquad \text{(A5)}\end{aligned}$$

where $\overline{A}_{ij}=\overline{k}_p\text{sech}(\overline{k}_p x_e)A_{ij}$ for $i=1, 1\le j\le 2$ and $\overline{A}_{ij}=\overline{k}_p\text{sech}(\overline{k}_p y_e)A_{ij}$ for $i=2, 1\le j\le 2$. Substitution of (A5) into (A1) gives

$$\dot{u}_{\text{pseudo}} = \overline{U}_{\zeta_1}\zeta_1+\overline{U}_{\zeta_2}\zeta_2+\overline{U}_{\overline{E}_u}\overline{E}_u+\overline{U}_{y_u}y_u+\overline{U}_C \qquad \text{(A6)}$$

where

$$\begin{aligned}\overline{U}_{\zeta_1} =& U_{\zeta_1}-U_{\dot{\zeta}_1}k_p\overline{k}_p\text{sech}(\overline{k}_p x_e)\\ \overline{U}_{\zeta_2} =& U_{\zeta_2}-U_{\dot{\zeta}_2}k_p\overline{k}_p\text{sech}(\overline{k}_p y_e)\\ \overline{U}_{\overline{E}_u} =& U_{\dot{\zeta}_1}\overline{A}_{11}+U_{\dot{\zeta}_2}\overline{A}_{21}\\ \overline{U}_{y_u} =& U_{\dot{\zeta}_1}\overline{A}_{12}+U_{\dot{\zeta}_2}\overline{A}_{22}\\ \overline{U}_C =& U_C+\begin{pmatrix}U_{\dot{\zeta}_1} & U_{\dot{\zeta}_2}\end{pmatrix}\begin{pmatrix}\cos(\psi_d) & -\sin(\psi_d)\\ \sin(\psi_d) & \cos(\psi_d)\end{pmatrix}\\ &\cdot\begin{pmatrix}-\sin(E_\psi/2) & -\cos(E_\psi/2)\\ \cos(E_\psi/2) & -\sin(E_\psi/2)\end{pmatrix}\\ &\times\begin{pmatrix}\overline{k}_p\text{sech}(\overline{k}_p x_e)U_{\dot{\zeta}_1}\overline{X}\\ \overline{k}_p\text{sech}(\overline{k}_p y_e)U_{\dot{\zeta}_2}\overline{Y}\end{pmatrix}\cdot 2\sin(E_\psi/2) \qquad \text{(A7)}\end{aligned}$$

are bounded, and the upper bounds are given by

$$\begin{aligned}&\left|\overline{U}_{\zeta_1}\right|,\ \left|\overline{U}_{\zeta_2}\right|\le\overline{U}_{\zeta\max}:=k_p r_{\max}+k_p^2\overline{k}_p \qquad \text{(A8a)}\\ &\left|\overline{U}_{\overline{E}_u}\right|,\ \left|\overline{U}_{y_u}\right|\le\overline{U}_{E_u}:=2k_p\cdot\max(1,r_{\max})\\ &\qquad\cdot(1+m_1 r_{\max}/d_2). \qquad \text{(A8b)}\end{aligned}$$

Next, by using (21b), (A4), (48), and (28b), the time derivative of r_{pseudo} in (22) becomes

$$\begin{aligned}\dot{r}_{\text{pseudo}} &= -(k_\psi/2)\cdot\cos(\overline{E}_\psi/2)\dot{\overline{E}}_\psi - \cos(y_\psi)\dot{y}_\psi/T_\psi \\ &= -(k_\psi/2)\cdot\cos(\overline{E}_\psi/2)\dot{\overline{E}}_\psi + \cos(y_\psi)\sin(y_\psi)/T_\psi^2 \\ &\quad - \cos(y_\psi)\dot{\psi}_{\text{pseudo}}/T_\psi \\ &= \left(k_\psi^2/2\right)\cdot\sin(\overline{E}_\psi/2)\cos(\overline{E}_\psi/2) - (k_\psi/2) \\ &\quad \cdot\cos(\overline{E}_\psi/2)(\overline{E}_r + y_r) + \cos(y_\psi)\sin(y_\psi)/T_\psi^2 \\ &\quad - \cos(y_\psi)\dot{\psi}_{\text{pseudo}}/T_\psi \\ &\le \overline{R}_{\overline{E}_\psi}\overline{E}_\psi + \overline{R}_{\overline{E}_r}\overline{E}_r + \overline{R}_{y_r}y_r + \overline{R}_C \end{aligned} \tag{A9}$$

where

$$\begin{aligned}&\overline{R}_{\overline{E}_\psi} = \left(k_\psi^2 2\right)\cdot\sin(\overline{E}_\psi/2)\cos(\overline{E}_\psi/2)/\overline{E}_\psi \\ &\overline{R}_{\overline{E}_r} = -(k_\psi/2)\cdot\cos(\overline{E}_\psi/2),\quad \overline{R}_{y_r} = -(k_\psi/2)\cdot\cos(\overline{E}_\psi/2) \\ &\overline{R}_C = \cos(y_\psi)\sin(y_\psi)/T_\psi^2 - \cos(y_\psi)/T_\psi. \end{aligned} \tag{A10}$$

are bounded and the upper bounds are given by

$$\begin{aligned}&\left|\overline{R}_{\overline{E}_\psi}\right| \le k_\psi^2/4,\quad \left|\overline{R}_{\overline{E}_r}\right| \le k_\psi/2,\quad \left|\overline{R}_{y_r}\right| \le k_\psi/2, \\ &\left|\overline{R}_C\right| \le 1/T_\psi^2 + |\dot{\psi}_{\text{pseudo}}|/T_\psi. \end{aligned} \tag{A11}$$

REFERENCES

[1] I. Kolmanovsky and N. H. McClamroch, "Developments in non-holonomic control problems," *IEEE Control Syst. Mag.*, vol. 15, no. 6, pp. 20–36, Dec. 1995.

[2] R. W. Brockett, "Asymptotic stability and feedback linearization," in *Differential Geometric Control Theory*, R. W. Brockett, R. S. Millman, and H. J. Sussman, Eds. Boston, MA: Birkhauser, 1983, pp. 181–191.

[3] Z.-P. Jiang and H. Nijmeijer, "Tracking control of mobile robots: A case study in backstepping," *Automatica*, vol. 33, no. 7, pp. 1393–1399, Jul. 1997.

[4] T.-C. Lee, K.-T. Song, C.-H. Lee, and C.-C. Teng, "Tracking control of unicycle-modeled mobile robots using a saturation feedback controller," *IEEE Trans. Control Syst. Technol.*, vol. 9, no. 2, pp. 305–318, Mar. 2001.

[5] P. Encarnação and A. Pascoal, "Combined trajectory tracking and path following control for dynamic wheeled mobile robots," in *Proc. 15th IFAC World Congress Autom. Control*, Barcelona, Spain, Jul. 2002.

[6] J.-M. Coron and E.-Y. Kerai, "Explicit feedback stabilizing of the attitude of a rigid spacecraft with two control torques," *Automatica*, vol. 32, no. 5, pp. 669–677, May 1996.

[7] H. Krishnan, M. Reyhanoglu, and H. McClamroch, "Attitude stabilization of a rigid spacecraft using gas jet actuators operating in a failure mode," in *Proc. 31st IEEE Conf. Decision Control*, 1992, pp. 1612–1617.

[8] H. Krishnan, M. Reyhanoglu, and N. H. McClamroch, "Attitude stabilization of a rigid spacecraft using two control torques: A nonlinear control approach based on the spacecraft attitude dynamics," *Automatica*, vol. 30, no. 6, pp. 1023–1027, Jun. 1994.

[9] P. Morin and C. Samson, "Time-varying feedback stabilization of the attitude of a rigid spacecraft with two controls," *Syst. Control Lett.*, vol. 25, no. 5, pp. 375–385, Aug. 1995.

[10] P. Morin and C. Samson, "Time-varying exponential stabilization of a rigid spacecraft with two control torques," *IEEE Trans. Autom. Control*, vol. 42, no. 4, pp. 528–534, Apr. 1997.

[11] M. Reyhanoglu, "Exponential stabilization of an underactuated autonomous surface vessel," *Automatica*, vol. 33, no. 12, pp. 2249–2254, Dec. 1997.

[12] R. Pettersen and O. Egeland, "Exponential stabilization of an underactuated surface vessel," *Modeling, Identif., Control*, vol. 18, no. 3, pp. 239–248, Jul. 1997.

[13] J. M. Godhavn, T. I. Fossen, and S. P. Berge, "Nonlinear and adaptive backstepping designs for tracking control of ships," *Int. J. Adaptive Control Signal Process.*, vol. 12, no. 8, pp. 649–670, Dec. 1998.

[14] K. Y. Pettersen and H. Nijmeijer, "Underactuated ship tracking control: Theory and experiments," *Int. J. Control*, vol. 74, no. 14, pp. 1435–1446, 2001.

[15] E. Lefeber, "Tracking control of nonlinear mechanical systems," Ph.D. dissertation, Dept. Appl. Math., University of Twente, Twente, The Netherlands, 2000.

[16] E. Lefeber, K. Y. Pettersen, and H. Nijmeijer, "Tracking control of an underactuated ship," *IEEE Trans. Control Syst. Technol.*, vol. 11, no. 1, pp. 52–61, Jan. 2003.

[17] Z. P. Jiang, "Global tracking control of underactuated ships by Lyapunov's direct method," *Automatica*, vol. 38, no. 2, pp. 301–309, Feb. 2002.

[18] K. D. Do, Z. P. Jiang, and J. Pan, "Underactuated ship global tracking under relaxed conditions," *IEEE Trans. Autom. Control*, vol. 47, no. 9, pp. 1529–1536, Sep. 2002.

[19] A. Behal, D. M. Dawson, W. E. Dixon, and Y. Fang, "Tracking and regulation control of an underactuated surface vessel with nonintegrable dynamics," *IEEE Trans. Autom. Control*, vol. 47, no. 3, pp. 495–500, Mar. 2002.

[20] K. D. Do, Z. P. Jiang, and J. Pan, "Universal controllers for stabilization and tracking of underactuated ships," *Syst. Control Lett.*, vol. 47, no. 4, pp. 299–317, Nov. 2002.

[21] K. D. Do, Z. P. Jiang, and J. Pan, "Robust adaptive path following of underactuated ships," *Automatica*, vol. 40, no. 6, pp. 929–944, Jun. 2004.

[22] Z.-P. Jiang and H. Nijmeijer, "A recursive technique for tracking control of nonholonomic systems in chained form," *IEEE Trans. Autom. Control*, vol. 44, no. 2, pp. 265–279, Feb. 1999.

[23] D. Wang and C. B. Low, "Modeling and analysis of skidding and slipping in wheeled mobile robots: Control design perspective," *IEEE Trans. Robotics*, vol. 24, no. 3, pp. 676–687, Jun. 2008.

[24] D. Swaroop, J. K. Hedrick, P. P. Yip, and J. C. Gerdes, "Dynamic surface control for a class of nonlinear systems," *IEEE Trans. Autom. Control*, vol. 45, no. 10, pp. 1893–1899, Oct. 2000.

[25] A. R. Girard and J. K. Hedrick, "Dynamic positioning of ships using nonlinear dynamic surface control," in *Proc. 5th IFAC Symp. Nonlinear Control Syst.*, St. Petersburg, Russia, 2001.

[26] H. Sira-Ramirez and S. K. Agrawal, *Differentially Flat Systems*. New York: Marcel Dekker, 2004.

[27] T. I. Fossen, *Guidance and Control of Ocean Vehicles*. Chichester, U.K.: Wiley, 1994.

[28] R. Sepulchre, M. Jankovic, and P. Kokotovic, *Constructive Nonlinear Control*. Berlin, Germany: Springer-Verlag, 1997.

[29] H. K. Khalil, *Nonlinear Systems*, 3rd ed. Englewood Cliffs, NJ: Prentice-Hall, 1996.

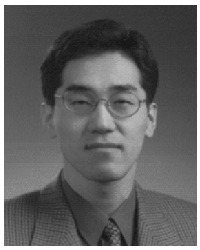

Dongkyoung Chwa received the B.S. and M.S. degrees in control and instrumentation engineering and Ph.D. degree in electrical and computer engineering from Seoul National University, Seoul, Korea, in 1995, 1997, and 2001, respectively.

From 2001 to 2003, he was a Post-Doctoral Researcher with Seoul National University, Seoul, Korea. In 2003, he was a Visiting Research Fellow with The University of New South Wales at Australian Defence Force Academy and an Honorary Visiting Academic with the University of Melbourne, Melbourne, Australia. In 2004, he was a BK21 Assistant Professor with Seoul National University. Since 2005, he has been with the Department of Electrical and Computer Engineering, Ajou University, Suwon, Korea, where he is currently an Associate Professor. His research interests are nonlinear, robust, and adaptive control theories and their applications to the robotics, underactuated systems including wheeled mobile robots, underactuated ships, cranes, and guidance and control of flight systems.